PROCEEDINGS OF THE ROYAL SOCIETY A MATHEMATICAL, PHYSICAL & ENGINEERING SCIENCES

Overtopping of solitary waves and solitary bores on a plane beach

T. E. Baldock, D. Peiris and A. J. Hogg

Proc. R. Soc. A 2012 **468**, 3494-3516 first published online 18 July 2012
doi: 10.1098/rspa.2011.0729

PROCEEDINGS OF THE ROYAL SOCIETY A

CrossMark click for updates

Proc. R. Soc. A (2012) **468**, 3494–3516
doi:10.1098/rspa.2011.0729
Published online 18 July 2012

Overtopping of solitary waves and solitary bores on a plane beach

By T. E. Baldock[1,*], D. Peiris[1] and A. J. Hogg[2]

[1]*School of Civil Engineering, University of Queensland, St Lucia, Queensland 4072, Australia*
[2]*Centre for Environmental and Geophysical Flows, School of Mathematics, University of Bristol, University Walk, Bristol BS8 1TW, UK*

The overtopping of solitary waves and bores present major hazards during the initial phase of tsunami inundation and storm surges. This paper presents new laboratory data on overtopping events by both solitary waves and solitary bores. Existing empirical overtopping scaling laws are found to be deficient for these wave forms. Two distinct scaling regimes are instead identified. For solitary waves, the overtopping rates scale linearly with the deficit in run-up freeboard. The volume flux in the incident solitary wave is also an important parameter, and a weak dependence on the nonlinearity of the waves (H/d) is observed. For solitary bores, the overtopping cannot be scaled uniquely, because the fluid momentum behind the incident bore front is independent of the bore height, but it is in close agreement with recent solutions of the nonlinear shallow water equations. The maximum overtopping rate for the solitary waves is shown to be the lower bound of the overtopping rate for the solitary bores with the same deficit in freeboard. Thus, for a given run-up, the solitary bores induce greater overtopping rates than the solitary waves when the relative freeboard is small.

Keywords: overtopping; solitary waves; solitary bores; tsunami; inundation

1. Introduction

Solitary waves are wave forms that consist of a single wave, rather than waves that form part of a series of continuous regular waves or random waves, the latter being typical of ocean wind and swell waves. Solitary-type waves occur over a range of geophysical scales, with the most well-known theoretical application being for tsunami waves generated by submarine seabed displacement or impulsive waves generated by landslides or asteroid impact (Synolakis & Bernard 2006). Solitary and single waves are also generated by vessel motion, particularly fast ferries (Russel 1845; Parnell & Kofoed-Hansen 2001), and can also be forced by transient wave groups (Baldock 2006), although there may be more than one solitary-type wave in a short group. If the solitary wave has sufficient magnitude it may run-up and overtop natural beach dunes and coastal defences such as breakwaters and seawalls, with potentially catastrophic effects for coastal infrastructure and populations (Borrero 2005; Wood & Bateman 2005). Solitary waves have

*Author for correspondence (t.baldock@uq.edu.au).

Received 14 December 2011
Accepted 21 June 2012

been very widely adopted to study long-wave run-up in laboratory experiments (Hall & Watts 1953; Synolakis 1987; Yeh *et al.* 1996; Li & Raichlen 2002; Chang *et al.* 2009), frequently for comparison with analytical and numerical models for tsunami warning and penetration, and to study the run-up of solitary bores (Baldock *et al.* 2009). This study aims to extend this approach to study the overtopping induced by such waves.

While solitary waves have long been used to represent tsunamis, Madsen *et al.* (2008) show that this is not likely to be usually the case because the geophysical scales over which tsunami propagate do not allow solitary waves to evolve and thus the link between wave height and wavelength is not well justified. In addition, more complex tsunami wave shapes occur than the idealized solitary wave. Further, as witnessed both in the 2004 Indian Ocean Tsunami and in the 2011 Japanese Tsunami, close to the shore, the leading edge of a tsunami may disintegrate into undular bores that may steepen sufficiently to break and form very long surf bores compared with those formed by wind and swell waves. For this period of the flow, descriptions or solutions for the flow based on solitary bores are more appropriate (Yeh 1991, 2006), which are closely related to those for surf zone bores (Shen & Meyer 1963; Hibberd & Peregrine 1979). Nevertheless, solitary waves have formed the basis for the majority of tsunami modelling and engineering analysis (Goring 1979; Synolakis 1987; Yeh *et al.* 1996; Li & Raichlen 2002; Carrier *et al.* 2003; Borthwick *et al.* 2006). Further, while solitary waves are typically steeper than tsunami (Madsen *et al.* 2008), for non-breaking waves the run-up mechanisms remain similar, with variations in the vertical run-up and flow velocity well described by the surf similarity parameter and wave steepness (Madsen & Fuhrman 2008). This study of the overtopping of solitary waves therefore complements the extensive literature on this topic, and provides the further advantage that the theory and scaling for solitary wave run-up is well known.

In addition to tsunami impacts, inundation of coastal zones and structures by overwash is a major hazard in many regions (Kobayashi 1999). In natural conditions, the run-up experiences a truncated beach if the run-up exceeds the beach crest, dune crest or structure crest, and then inundation by run-up induced overtopping occurs. However, while the run-up of solitary-type waves has been extensively studied, primarily for application to tsunami hazards (Yeh 1991, 2006; Kobayashi *et al.* 1998; Borthwick *et al.* 2006; Chang *et al.* 2009), and particularly for non-breaking waves, very little work has considered overtopping of solitary waves. No previous quantitative data describing the overtopping rates, and the scaling, of either non-breaking solitary waves or breaking solitary bores are available. Stansby (2003) developed an advanced Boussinesq model for run-up and overtopping of solitary waves that showed good agreement with the experimental data for run-up and flow depth, but no data were available for verification of predicted overtopping volumes. Hunt-Raby *et al.* (2011) compared the overtopping volumes of individual waves within a transient wave group with that from a single non-breaking solitary wave, and only for a single freeboard elevation. Further, no comparison of solitary wave overtopping has been made with traditional overtopping scaling laws for monochromatic or random waves (Hedges & Reis 2004; Goda 2009; van der Meer *et al.* 2009). Consequently, the scaling laws for solitary wave overtopping have not been identified, as they have been, for example, for solitary wave run-up.

This work investigates these issues, and presents the results of recent laboratory experiments measuring the overtopping flows from solitary waves and solitary bores on a sloping truncated beach. The aims are to investigate the differences in overtopping induced by solitary waves and solitary bores, to derive a scaling law for solitary wave overtopping and to test our recent solutions (Hogg *et al.* 2011) describing the overtopping rates for bores. This paper is organized as follows: §2 provides an overview of previous work on tsunami, overwash and overtopping of wave-run-up, together with an outline of the model for bore run-up and overtopping (Shen & Meyer 1963; Peregrine & Williams 2001; Guard & Baldock 2007; Hogg *et al.* 2011). Section 3 describes the experimental set-up, data collection and wave conditions in the experiments. The results, a new scaling law for solitary waves and comparisons with the Hogg *et al.* (2011) overtopping model are presented in §4. Final conclusions appear in §5.

2. Background

(*a*) *Previous studies*

An extensive summary of the literature on solitary wave propagation, run-up and impact in the context of tsunami impact is given by Synolakis & Bernard (2006). This work investigates the overtopping flow, which has not been extensively studied. Further, most previous work has focused on non-breaking waves impacting at the shoreline. Additionally, tsunami waves, or the leading positive waves in a tsunami wave train, may also make landfall in the form of broken waves or bores, which impact coastal defences and beaches, and lead to the initial overwash or overtopping of coastal dunes and seawalls. Eventually, the large mass of water in the main tsunami wave overtakes the initial bore-driven run-up, generally leading to further inundation. However, during the initial first few minutes, the impact of the tsunami may be dominated by the run-up from broken waves or bores. This initial period is important in the context of human safety on the immediate foreshore and in terms of warning systems and evacuation strategies. It is also relevant to the potential impact forces on structures, particularly if the run-up picks up debris along the coastline (Yeh 2006).

Early tsunami observations were frequently interpreted as turbulent bores (Synolakis & Bernard 2006), and turbulent bores also represent a common shoreline condition during storm, cyclone and hurricane overtopping. Peregrine (1966, 1967) formulated solutions to the depth-averaged nonlinear shallow water equations (NLSWEs) that describe both the propagation and run-up of such bores. Further work by Hibberd & Peregrine (1979) provided numerical solutions for the overland or swash flows for long bores. This complemented the earlier theoretical work of Shen & Meyer (1963), which provides an asymptotic solution for the hydrodynamics in the swash zone close to the wave tip. The solutions of the NLSWE model the run-up of long waves and bores, from which overtopping flow volumes can be determined, together with the hydrodynamics in the inundation zone. For non-breaking solitary waves, analytical solutions are relevant to this study (Synolakis 1987; Carrier *et al.* 2003), but to the authors' knowledge, these have not been applied to describe overwash or overtopping volumes. Previous

work has considered the classical analytical solution of Shen & Meyer (1963) to describe bore run-up and overtopping due to run-up, or swash overtopping (Peregrine & Williams 2001). However, recent new solutions to the NLSWE (Guard & Baldock 2007; Pritchard *et al.* 2008; Antuono & Hogg 2009) show that the Shen & Meyer solution is not conservative for engineering design, and that it significantly underestimates flow depths and overtopping flow volumes. This had been identified in earlier experiments by Baldock *et al.* (2005), which prompted the development of the new solutions. Given that the usual criterion for human safety during flood events is based on a product of water depth and flow velocity (Ramsbottom *et al.* 2003), and that the forces on structures are proportional to the momentum flux, a product of the velocity squared and depth, the underestimation of flow depths by the traditional model can lead to significant underestimation of potential hazards from bore run-up.

Numerical modelling of wave overwash over steep coastal structures has used a wide range of techniques, from nonlinear shallow water wave models (Kobayashi & Wurjanto 1989; Dodd 1998) to Boussinesq models (Stansby 2003; Orszaghova *et al.* 2012), Navier–Stokes solvers (Ingram *et al.* 2009) and smooth particle hydrodynamics models (Dalrymple & Rogers 2006). A number of empirical formulae are also available (Goda 2009; van der Meer *et al.* 2009), although these are more applicable for sequences of periodic or random waves. On natural beaches, sand dunes and beach berms provide the first line of coastal defence, and overtopping leads to flooding of the backshore as well as the transport and deposition of marine sand and saline water (Kobayashi *et al.* 1996). For extreme conditions, when storm surge elevations exceed the berm crest, wave overtopping may combine with a steady flood flow (Hughes & Nadal 2009), and berm rollover and breaching of the barrier may occur. Overviews of these processes are given by Kraus *et al.* (2002) and Donnelly *et al.* (2006). Similar processes may occur owing to tsunami overtopping and subsequent drawdown. Overtopping of beach berms is particularly important in determining the sediment overwash and deposition, and hence the berm growth during both modal and extreme wave conditions (Hine 1979; Nott 2003; Weir *et al.* 2006).

(*b*) *Bore overtopping model*

To date, no analytical theory exists for the overtopping of non-breaking or breaking solitary waves. However, while such a description appears possible by combining the theoretical work of Carrier *et al.* (2003) and Hogg *et al.* (2011), this is left for future work. To describe the overtopping of bores, models of the run-up due to breaking waves are instructive and are usually built upon the assumption that the pressure is hydrostatic and the motion modelled by the NLSWE. In this context, the dimensionless one-dimensional shallow water equations over a planar beach are given by

$$\frac{\partial h}{\partial t}+\frac{\partial}{\partial x}(uh)=0 \quad \text{and} \quad \frac{\partial u}{\partial t}+u\frac{\partial u}{\partial x}+\frac{\partial h}{\partial x}+1=0, \tag{2.1}$$

where $h(x,t)$ denotes the height of the shallow layer, which flows with velocity $u(x,t)$. The system has been rendered dimensionless by a vertical lengthscale h_0, a horizontal lengthscale $h_0/\tan\gamma$, and a time scale $(h_0/g)^{1/2}/\tan\gamma$, where h_0 is chosen so that the maximum run-up reaches a height $2h_0$ above the still water

level and γ is the beach gradient. Shen & Meyer (1963) derived a simple solution for run-up, which captures asymptotically the form of the velocity and height fields close to the wave-tip for general conditions. This solution may be thought of as a dam-break wave up a slope, where the water behind the dam is initially stationary and sloping parallel to the bed and has been treated as capturing the entire swash-generated run-up (Peregrine & Williams 2001; Pritchard & Hogg 2005). However, the Shen & Meyer solution advects only a relatively small volume of fluid forward from the collapsing bore and is found to be inappropriate for many surf-zone bores (Baldock *et al.* 2005). Recognizing the significance of the mass and momentum fluxes behind the bore, Guard & Baldock (2007) computed numerical solutions to the NLSWE, on the basis of different boundary conditions that prescribed more realistic off-shore conditions. These solutions were subsequently encapsulated in a compact analytical form by Pritchard *et al.* (2008).

The Peregrine & Williams (2001) and Guard & Baldock (2007) solutions specifically exploit the hyperbolic structure of the NLSWE and decompose the system into a characteristic form. They identify dimensionless characteristic quantities, $\alpha = u + 2\sqrt{h} + t$ and $\beta = u - 2\sqrt{h} + t$, which are conserved on the characteristics $\mathrm{d}x/\mathrm{d}t = u \pm \sqrt{h}$, respectively. Their boundary conditions comprise setting $\alpha = 2 + kt$, on the characteristics $\beta = -2/3$, where k is a positive constant. The characteristic $\beta = -2/3$ emanates from the origin and initially remains tangent to $x = 0$; it may be thought of as the seaward extent of the collapsing bore. The parameter k determines the magnitude of the mass and momentum fluxes behind the bore. The case $k = 0$ corresponds to the Shen & Meyer (1963) solution, while as k is increased the bore is sustained more strongly, and Guard & Baldock (2007) demonstrated that $k = 1$ gave reasonably good agreement with experimental measurements of the flow depth within the swash zone. Power *et al.* (2011) have recently verified that this model describes the swash zone flow patterns during the run-up of natural surf zone bores on a variety of beaches. It is worth reiterating that the maximum run-up is independent of the parameter k. However, increases in k lead to solutions that have a longer duration of inflow across the original still water shoreline, later times of flow reversal, increased depths in the swash and a more symmetric velocity field between uprush and backwash (Guard & Baldock 2007; Pritchard *et al.* 2008).

Following the approach of Peregrine & Williams (2001), who adopted the Shen & Meyer model, Hogg *et al.* (2011) developed further semi-analytical solutions for the overtopping flows induced by the wave forms proposed by Guard & Baldock (2007). This model of overtopping is based upon the end of the beach acting as a point of hydraulic control where the local Froude number is at least unity. During the initial phases of the inrush, the motion is supercritical and thus unaffected by the overtopping at the end of the beach. However as the flow deepens and slows, the hydraulic control becomes significant and alters the subsequent motion. Hogg *et al.* (2011) demonstrated that the results built on the Shen & Meyer (1963) model of motion lead to much smaller predictions of overtopping volumes. This reflects the observations above that the Shen & Meyer description, if treated as modelling the entire swash rather than just the asymptotic solution close to the wave-tip, leads to too little mass and momentum being advected shorewards. Hogg *et al.* (2011) showed how that overtopping volume may be calculated from a semi-analytical solution, which is evaluated through relatively simple numerical quadrature. Their results illustrate how the

parameter k determines the magnitude of the overtopping volume; for example, the predicted volume varies by a factor of close to 3 as k increases from 0 to 1. It is noteworthy that all the solutions correspond to waves that have the same run-up magnitude. Thus, the changes in overtopping volumes for different values of k are not a result of larger bore amplitudes or greater run-up; they result from different mass and momentum flux behind the breaking front of the incident bore. Consequently, bores with the same height and run-up can generate very different overtopping rates. The implications of this are particularly important when considering scaling laws for the overtopping of breaking waves.

(*c*) *Empirical overtopping laws*

Typical empirical overtopping scaling laws derived from data or dimensional analysis take the form (see, for example, van der Meer *et al.* 2009):

$$q = f\left(\frac{z}{H}, X\right), \tag{2.2}$$

where q is the dimensional overtopping volume per unit width of beach, H is the wave height at the toe of the beach or structure, z is the elevation (freeboard) of the structure or beach crest relative to the still water level or structure toe and X is a set of further parameters such as wave period, wave height, structure geometry, roughness, wave direction, water depth, etc. Hedges & Reis (2004) use the maximum run-up in place of the wave height in their similar random wave model.

Given the theory of Guard & Baldock (2007) and Hogg *et al.* (2011), such scaling, based largely on relative crest elevation (z/H or z/R), cannot describe the overtopping of solitary bores or surf zone bores because the wave height or run-up is not the sole controlling parameter. This is verified experimentally below. Further, we find that such scaling is also inadequate in describing the overtopping of solitary waves, and derive a new scaling law based on the deficit in freeboard (see §3) with respect to the run-up elevation on a non-truncated slope and the volume flux in the incident wave, rather than using the ratio of freeboard to wave height.

3. Experimental set-up

(*a*) *Wave flume and instrumentation*

The overtopping experiments were conducted in a 0.85 m wide, 0.75 m deep and 28 m long wave flume in the Hydraulics Laboratory at the University of Queensland. The bathymetry comprised a 10.5 m long horizontal section from the wavemaker to the toe of a uniform long sloping beach of gradient $\gamma = 0.107$ (figure 1). The sloping beach was constructed in two parts: a fixed lower section below the still water line (SWL), which is the position of the initial shoreline, and an adjustable beach with removable panels above the SWL. The origin of the horizontal coordinate is at the SWL and positive onshore. The surface of the beach was a smooth painted marine plywood bed. Joints between adjacent panels were sanded flush to minimize additional roughness. Following previous studies (Baldock *et al.* 2005), the removable panels on the upper beach could be

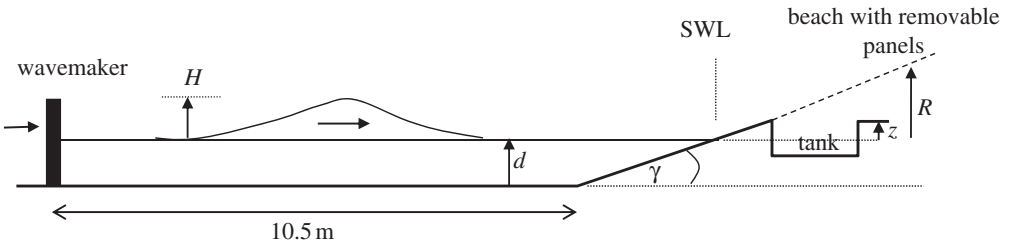

Figure 1. Schematic of experimental layout.

interchanged with an overtopping tank sunk within the bed at different elevations relative to the SWL and the maximum run-up. A special tank was designed, which encompassed the middle two-thirds of the flume to avoid wall effects, and which also included thin 'wing' walls to prevent flow from entering from the sides. The tank was 0.55 m in length, 0.45 m in width and 0.195 m deep, and resulted in a truncated beach at the seaward, or offshore, edge of the tank, which represents an idealized structure, berm or dune crest. The experiments were performed with the overtopping tank located at six locations along the beach, truncating the beach at $z = 0.05$–0.26 m above the SWL. The water depth over the horizontal section of the flume was also varied between $d = 0.105$–0.26 m; this additionally changed the beach truncation position relative to the SWL.

The natural run-up elevation, R, was determined visually for each wave condition by running the identical wave condition with a non-truncated beach and without the tank. Overtopping volumes per unit width were measured in the tank, using an ultrasonic distance sensor to measure the surface elevation change between the start and end of the test, with a calibrated conversion function to account for small differences in tank area with water surface elevation. Surface elevation was measured at a number of locations along the flume using ultrasonic displacement sensors with an absolute accuracy better than 1 mm and a relative accuracy of order 0.2 mm. For the present work, only the measurements at the toe of the sloping beach and SWL are required, which provide the offshore or incident wave height, H and flow depths at the lower boundary of the swash zone. The elevation of the truncated beach, z, represents the freeboard above the SWL. The deficit in freeboard is defined as R–z, i.e. the additional elevation required to prevent overtopping.

(*b*) *Wave conditions*

Solitary waves and solitary bores were generated using a computer-controlled hydraulic piston wavemaker that has stroke lengths of up to 1.4 m to generate long bores. Solitary waves that did not break before reaching the shore were generated using the wavemaker trajectory functions of Goring & Raichlen (1980). Large solitary waves that broke and formed bores over the sloping beach were also generated by this method. An error function signal was additionally adopted to generate breaking bores, following previous investigations of the kinematics within breaking solitary waves (Baldock *et al.* 2009). The latter function does not maintain the link between the wavelength and the wave-height-to-depth ratio

(H/d) that holds for solitary waves and the waves generated are termed single waves as opposed to solitary waves (Madsen & Schaffer 2010). The wavemaker motion and resulting wave forms are very repeatable, enabling the use of multiple tank positions and repeat runs of the same wave form. Example wavemaker displacement functions and resulting waveforms are given in Seelam *et al.* (2011).

Two wave types are distinguished in this study: solitary waves and solitary bores. The latter are single waves that broke prior to reaching the SWL. The solitary waves generally broke onto the beach face, and did not form breaking bores prior to reaching the still water shoreline. This distinction was made through careful visual observation for each case. In the constant depth region of the flume, wave heights ranged from 2 to 16 cm, with run-up elevations ranging from 6 to 32 cm (table 1). The range of wave height and water depth lead to a minimum value of $H/d\gamma^{10/9} = 1.44$. This wave was observed to break during the run-down phase but not during the run-up. This value is 75 per cent greater than the theoretical steepness at the onset of solitary wave breaking during the run-up ($H/d\gamma^{10/9} > 0.818$), as derived by Synolakis (1987) and Madsen & Schaffer (2010). However, it should be noted that the experimental data of Synolakis (1987) indicate that the onset of solitary wave breaking occurred at $H/d\gamma^{10/9} = 1.52$, and the numerical calculations of Borthwick *et al.* (2006) indicate even larger values. Consequently, these data are consistent with previous data but also indicate that the (inviscid) theoretical solution underestimates the relative wave steepness at the onset of breaking. All other waves broke either at the shore or formed bores during propagation along the flume or over the sloping beach. Smaller solitary waves were avoided to minimize frictional effects during the run-up and overtopping. Direct measurements of bed shear stress for solitary waves (Seelam *et al.* 2011) and solitary wave run-up (Barnes *et al.* 2009) in this same wave flume over a smooth bed and with a similar beach slope give friction factors of order $f = 0.015$ and $f = 0.02$, respectively. Frictional effects are significant at the run-up tip, where the water depth is very shallow, but less important in the body of the flow. Altogether, 15 different wave conditions were used, repeated for four different water depths and six different (in absolute elevation) tank positions (table 1). Not every wave condition induced overtopping at the higher truncation elevations, and some combinations of wave condition and low truncation elevation induced overtopping volumes that exceeded the tank capacity; these were excluded from the analysis.

The wave conditions were selected so that, for a given depth, the solitary bores generated with different wavemaker stroke length induced very similar wave heights and run-up elevations. Variations in overtopping volume between such sets of solitary waves are then a clear indication of the influence of the different boundary conditions proposed by Guard & Baldock (2007) and Hogg *et al.* (2011). Figure 2 shows the examples of the water surface elevation at the SWL for two solitary waves and two solitary bores plotted so the arrival time at the SWL is similar for each pair. Reflected waves have been removed for clarity. Each pair has a similar shape, particularly for the solitary waves. The two solitary bores have a very similar maximum surface elevation (wave height) and period, but the flow behind the bore front is sustained more strongly during case 13 than during case 8, such that large depths are maintained for longer, with greater inflow across the SWL. However, the run-up induced by each of these two solitary bores is very similar, 0.28 and 0.3 m, respectively.

Table 1. Wave conditions. d, water depth; H, wave height; z, truncation elevation; S, stroke length.

solitary waves				solitary bores				
case	d (cm)	H (cm)	z (cm)	case	d (cm)	S (cm)	H (cm)	z (cm)
1	26	3.2	9.1	7	26	0.59	14.6	9.1, 17.5, 26.1
2	26	4.1	9.1	8	26	0.67	14.7	9.1, 17.5, 26.1
3	26	6.1	9.1, 17.5	9	26	0.84	14.0	9.1, 17.5, 26.1
4	26	8.3	9.1, 17.5	10	26	1.04	15.6	17.5, 26.1
5	26	10.6	9.1, 17.5, 26.1	11	26	0.63	—	—
6	26	15.5	9.1, 17.5, 26.1	12	26	0.84	13.9	9.1, 17.5, 26.1
1	21	2.9	6.2	13	26	1.04	14.9	17.5, 26.1
2	21	3.7	6.2, 14.6	14	26	1.26	14.6	17.5, 26.1
3	21	5.6	6.2, 14.6	15	26	1.38	15.5	17.5, 26.1
4	21	7.6	6.2, 14.6	7	21	0.59	12.7	6.2, 14.6, 23
5	21	9.8	6.2, 14.6,23	8	21	0.67	11.8	6.2, 14.6, 23
1	15.5	2.5	4.2	9	21	0.84	11.5	6.2, 14.6, 23
2	15.5	3.4	4.2	10	21	1.04	12.1	14.6, 23
3	15.5	5.1	4.2, 12.7	11	21	0.63	14.0	6.2, 14.6, 23
4	15.5	7.4	4.2, 12.7	12	21	0.84	12.3	6.2, 14.6, 23
5	15.5	10.0	4.2, 12.7, 21.2	13	21	1.04	12.6	14.6, 23
1	10.5	2.2	5.3	14	21	1.26	12.6	14.6, 23
2	10.5	2.9	5.3	15	26	1.38	12.4	14.6, 23
3	10.5	4.6	5.3,9.5	7	15.5	0.59	10.1	4.2, 12.7, 21.2
4	10.5	6.1	5.3,9.5	8	15.5	0.67	9.1	4.2, 12.7, 21.2
5	10.5	6.7	5.3,9.5	9	15.5	0.84	9.4	4.2, 12.7, 21.2
				10	15.5	1.04	10.0	4.2, 12.7, 21.2
				11	15.5	0.63	9.8	4.2, 12.7, 21.2
				12	15.5	0.84	9.2	4.2, 12.7, 21.2
				13	15.5	1.04	8.9	4.2, 12.7, 21.2
				14	15.5	1.26	9.6	4.2, 12.7, 21.2
				15	15.5	1.38	9.8	4.2, 12.7, 21.2
				7	10.5	0.59	6.4	5.3,9.5
				8	10.5	0.67	6.2	5.3, 9.5
				9	10.5	0.84	6.8	5.3, 9.5
				10	10.5	1.04	6.7	5.3, 9.5
				11	10.5	0.63	7.0	5.3, 9.5
				12	10.5	0.84	6.5	5.3, 9.5
				13	10.5	1.04	6.0	5.3, 9.5
				14	10.5	1.26	6.4	5.3, 9.5
				15	10.5	1.38	6.7	5.3, 9.5

4. Experimental results

(a) *Run-up of solitary waves*

The classical scaling of the run-up for both non-breaking and breaking solitary waves is quite similar and from both theory and experiment takes the form

$$\frac{R}{d} = \alpha \left(\frac{H}{d} \right)^{\beta}, \tag{4.1}$$

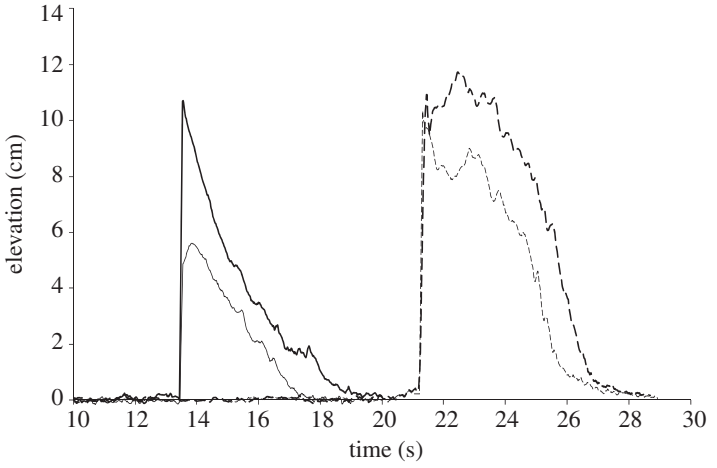

Figure 2. Example water surface elevations at the SWL, water depth $d = 26$ cm. Thin solid line, case 2; thick solid line, case 5; thin dashed line, case 8; thick dashed line, case 13. Reflected waves have been removed for clarity, and time axis adjusted for each pair such that the wavefronts coincide.

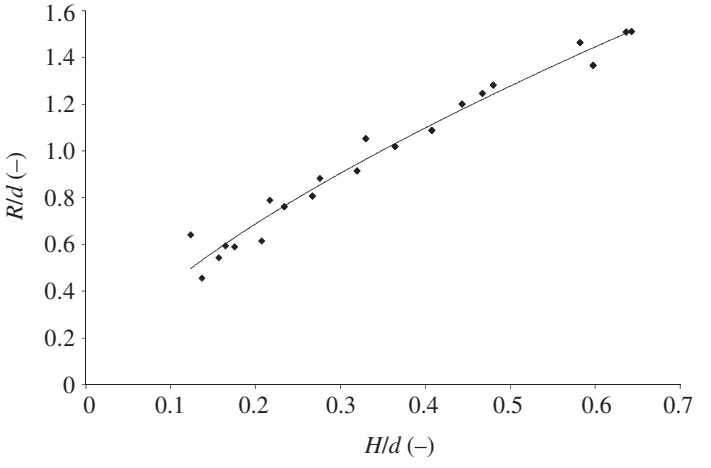

Figure 3. Normalized run-up versus normalized wave height at the beach toe, solitary waves. Solid line is $R/d = 2.04(H/d)^{0.68}$, $R^2 = 0.96$.

where α and β are empirical parameters that depend on beach slope, breaking conditions and frictional effects (Synolakis 1987; Li & Raichlen 2002; Borthwick *et al.* 2006; Madsen & Schaffer 2010). The present data are in very good agreement with this scaling, giving $\alpha = 2.04$ and $\beta = 0.68$, with an R^2 correlation coefficient of 0.96 (figure 3). Data for breaking waves on a 1 : 20 slope give $\alpha \approx 1$ and $\beta \approx 0.6$ (Synolakis 1987) and data and numerical modelling by Li & Raichlen (2002) and Borthwick *et al.* (2006) show that both α and β increase with increasing beach gradient, and α decreases as friction increases. For the present beach gradient of order 0.1, the numerical model results given in Borthwick *et al.* (2006) suggest $\alpha \approx 2$ and $\beta \approx 0.8$ when frictional effects are included (their fig. 6). Consequently, the present breaking solitary wave run-up data are very consistent with previous

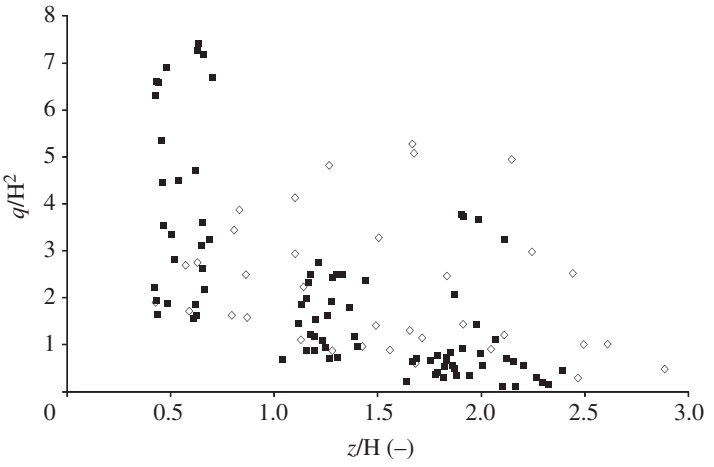

Figure 4. Conventional scaling showing significant data scatter: non-dimensional overtopping volume versus non-dimensional freeboard. Open diamonds, solitary waves; filled squares, bores.

experimental and numerical estimates, suggesting that the following overtopping data were derived from wave conditions very similar to those used to generate the extensive existing solitary wave run-up dataset.

(*b*) *Overtopping*

(i) *Conventional scaling*

Figure 4 presents the overtopping volumes per unit width (q) in the conventional format given by equation (2.1), which is widely adopted for empirical descriptions of overtopping rates for periodic and random waves. Data for both solitary waves and solitary bores are shown. The solitary wave data show significant scatter with this scaling, even though the data are all obtained for a single beach slope and roughness, and shore normal waves. The scatter is similar (if not larger) for the solitary bores, particularly for small relative freeboard, z/H. Indeed, for $z/H \approx 0.5$ the dimensionless overtopping volume varies by a factor of order five. Clearly, this scaling is unsatisfactory for both the solitary waves and solitary bores. Taking z/R as the abscissa does not change the scatter, and there is no significant change apart from a re-scaling of the axis, because the run-up is approximately linearly proportional to the wave height (i.e. $\beta = 0.8$ in equation (2.2)).

(ii) *Comparison between solitary waves and solitary bores*

Given the poor correlation of the data with equation (2.1), we investigate alternative scaling for the overtopping. A plot (figure 5) of dimensional overtopping volume, q (litres per metre width of beach crest) versus the non-truncated run-up, R, illustrates that the normal run-up elevation is a controlling parameter and that q increases linearly with R. The overtopping volume remains a function of the truncation elevation, z, and a weak function of the water depth, d. Considering data for just a single water depth, and removing the truncation

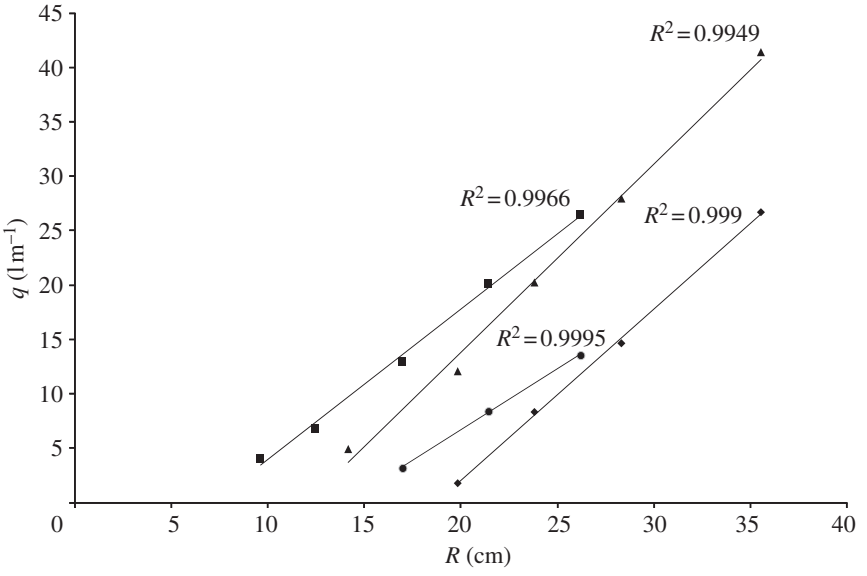

Figure 5. Dimensional overtopping volume versus run-up elevation for varying water depths and truncation elevation (d,z), solitary waves. Filled squares, (26, 9 cm); filled circles, (26, 17 cm); filled triangles, (21, 6 cm); filled diamonds, (21, 14 cm).

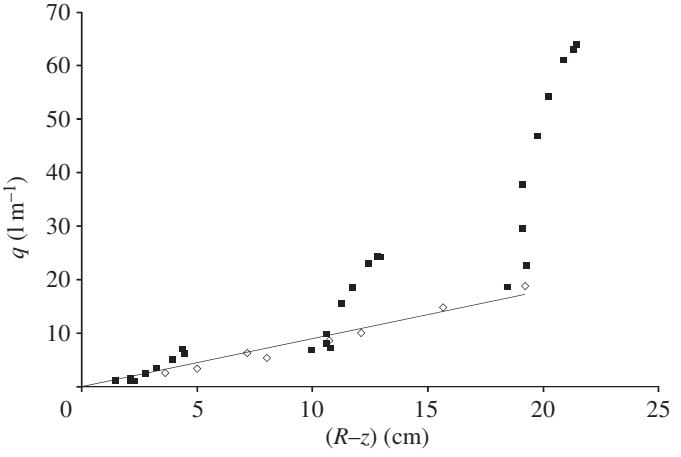

Figure 6. Dimensional overtopping volume as a function of deficit in freeboard for solitary waves and developed bores, $d = 15.5$ cm. Open diamonds, solitary waves; filled squares, bores. Solid line is $y = 0.9x$, $R^2 = 0.96$.

elevation by plotting q versus the deficit in run-up freeboard $(R–z)$ leads to a linear relationship between q and $(R–z)$, illustrated in figure 6. Also illustrated in figure 6 are the overtopping data for the solitary bores, again at this same single water depth. For the beach truncated close to the run-up limit, small $(R–z)$, the overtopping rate for both the solitary waves and solitary bores is very similar. However, for larger deficits in freeboard, the data for the bores show

a very different functional form, becoming independent of R and multi-valued at constant values of $(R–z)$. This is discussed further below, but is a direct consequence of the different inflow conditions identified by Guard & Baldock (2007). Further, figure 6 demonstrates that the maximum overtopping rate for the solitary waves is the lower bound of the overtopping rate for the solitary bores with the same freeboard deficit. Thus, for a given run-up, the solitary bores transport greater volumes of water across the SWL than the solitary waves and consequently induce greater overtopping rates when the relative freeboard is small.

(iii) *Scaling of the solitary wave overtopping*

The dimensional overtopping data are normalized by the theoretical volume flux transported across a fixed vertical plane by the incident solitary wave, q_o. This can be approximated from the theory for a solitary wave propagating over a horizontal bed:

$$q_o = \int_{-\infty}^{\infty} u(\eta + d)\mathrm{d}t \approx \sqrt{\left(\frac{4}{3}\right)^3 H^3 d} + \sqrt{\frac{16}{3} H d^3}, \tag{4.2}$$

where the long-wave velocity $u = c(\eta/d), \eta$ is the surface elevation of the solitary wave (Madsen & Schaffer 2010) and linear theory is used to approximate the wave speed, c. Further examination of the solitary wave data shows a weak dependence on the nonlinearity of the solitary waves, H/d, with an empirical relationship $q \propto (H/d)^{1/4}$, inspired by the dependence of the run-up on H/d as identified by Synolakis (1987). We suggest this dependence arises from the partioning of the volume flux into the two terms of different functional form in equation (4.1), corresponding to the mass transport above and below the SWL, respectively. Hence, two solitary waves with the same total volume flux in the offshore region can induce a different overtopping volume because the balance between the mass transport above and below the SWL is dependent on H and d. However, further data for other beach slopes and surface roughness would be required to rule out alternative explanations for this dependency. Given the work of Borthwick *et al.* (2006), a numerical investigation may prove useful in this respect.

It is useful to plot the abscissa in non-dimensional form $((R–z)/R)$ to eliminate the length scale of the run-up and to illustrate the dependence of the overtopping on the relative elevation of the truncation point within the run-up zone. Adopting this scaling and accounting for the nonlinearity of the wave form by plotting q/q_o versus $[(R - z)/R](H/d)^{1/4}$ shows an excellent correlation for the present data (figure 7). For a beach with this slope truncated at the SWL, the overtopping volume is approximately half of the volume flux in the incident wave. Clearly, this would lead to very significant overtopping volumes for large solitary-type waves. The correlation coefficient reduces slightly to 0.95 if the wave nonlinearity term, $(H/d)^{1/4}$, is excluded, but further work is required to determine the importance of this term for a wider range of H/d. Similarly, while much of the influence of the beach slope will be captured by scaling on the run-up, further work is required to identify if beach slope remains an independent parameter with this scaling.

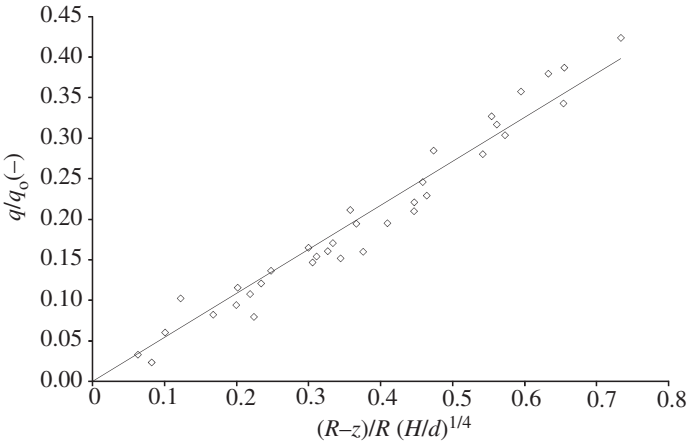

Figure 7. Normalized overtopping volume for various depths as a function of normalized deficit in freeboard and wave nonlinearity for solitary waves. Best fit line is $y = 0.54x$, $R^2 = 0.96$.

(iv) *Solitary bores*

The experiments were designed to generate solitary bores with similar heights for a range of different wavemaker stroke lengths. The solitary bore height close to the shore varies owing to both the initial height at the wavemaker and the dissipation along the flume and both are influenced by the water depth. However, the ratio H/d is not constant for the four water depths, indicating that the solitary bore height is not depth-limited. Figure 8*a* illustrates the variation of bore height at the toe of the beach for different stroke lengths and water depths. While the bore height varies with the water depth, it does not vary significantly with stroke. Similarly, the run-up varies with the water depth, but again varies little with stroke (figure 8*b*). For the bores, the maximum value of $R/d \approx 1.8$, which is similar to the upper limit of R/d observed for the solitary waves.

Following the scaling adopted by Peregrine & Williams (2001), the non-dimensional truncation point (edge) of the beach is written as $E = 2z/R_i$, where R_i is the maximum vertical run-up for inviscid wave conditions, and z is the elevation of the tank edge relative to the SWL. Hence, E ranges from zero (at the SWL) to two (at the run-up limit). The non-dimensional overtopping volume per unit width of beach, $V(E)$, is obtained from the measured dimensional overtopping volume, $V^*(E)$, following Peregrine & Williams (2001):

$$V(E) = \frac{V^*(E)\sin(2\gamma)}{2A^2}, \tag{4.3}$$

where $2A = R_i$ and γ is the beach gradient.

The scaling for this solution of the NLSWE is based on inviscid conditions. However, while the run-up tip is quite strongly affected by friction, where the flow depth is very small, the majority of the flow is much less affected by friction because flow depths are large and velocities are smaller. Consequently, the use of the measured values of the run-up elevation leads to estimated values for E that are too large. To address this, the period of the total swash motion was

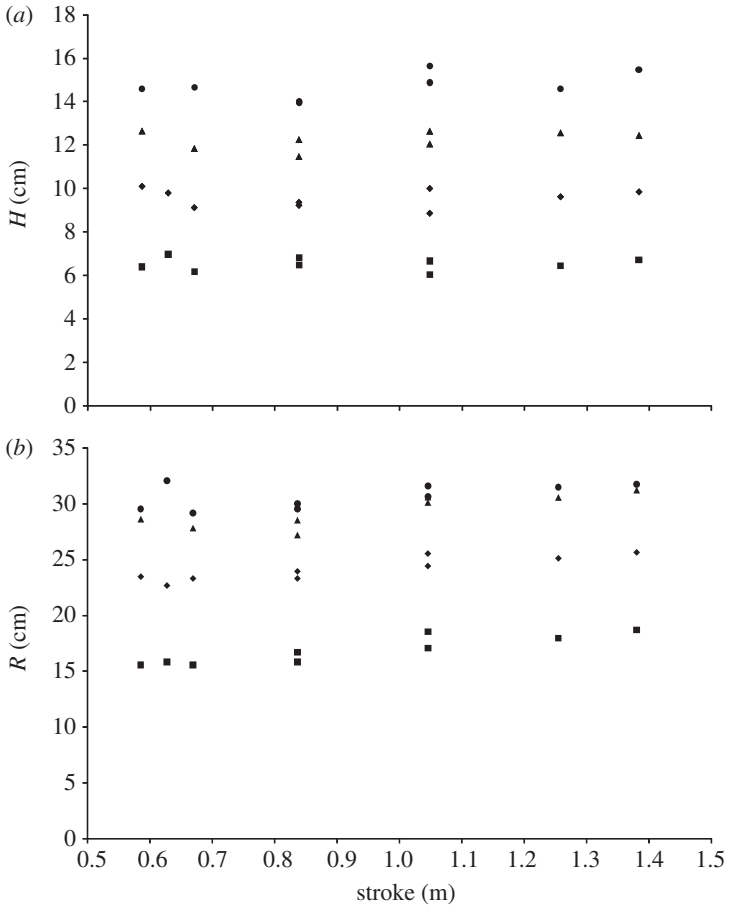

Figure 8. (*a*) Solitary bore height at beach toe versus wavemaker stroke length. Filled squares, $d = 10.5$ cm; filled diamonds, $d = 15.5$ cm; filled triangles, $d = 21$ cm; filled circles, $d = 26$ cm. (*b*) Solitary bore run-up versus wavemaker stroke length. Filled squares, $d = 10.5$ cm; filled diamonds, $d = 15.5$ cm; filled triangles, $d = 21$ cm; filled circles, $d = 26$ cm.

estimated from the flow depth measured at the SWL, which is expected to be less influenced by friction than the run-up tip. For the inviscid solution, the swash period and run-up elevation are directly related (Peregrine & Williams 2001), enabling an estimate of the theoretical inviscid run-up elevation. These calculations suggested that the measured run-up was approximately 75 per cent of the expected run-up for inviscid conditions. This ratio is in very close agreement with that given by previous studies (Meyer & Taylor 1972). For all cases, we thus adopt $R_\mathrm{i} = 1.33R$ and evaluate E, A and $V(E)$ accordingly from equation (4.2).

Adopting this scaling, the overtopping data for the bores are plotted in figure 9*a*, where the overtopping model of Peregrine & Williams (2001), denoted PW01, is also shown. At first glance, this scaling yields a poor correlation. However, there are clear clusters of data, where the overtopping volume is multi-valued for the same value of E, particularly for smaller values of E. This

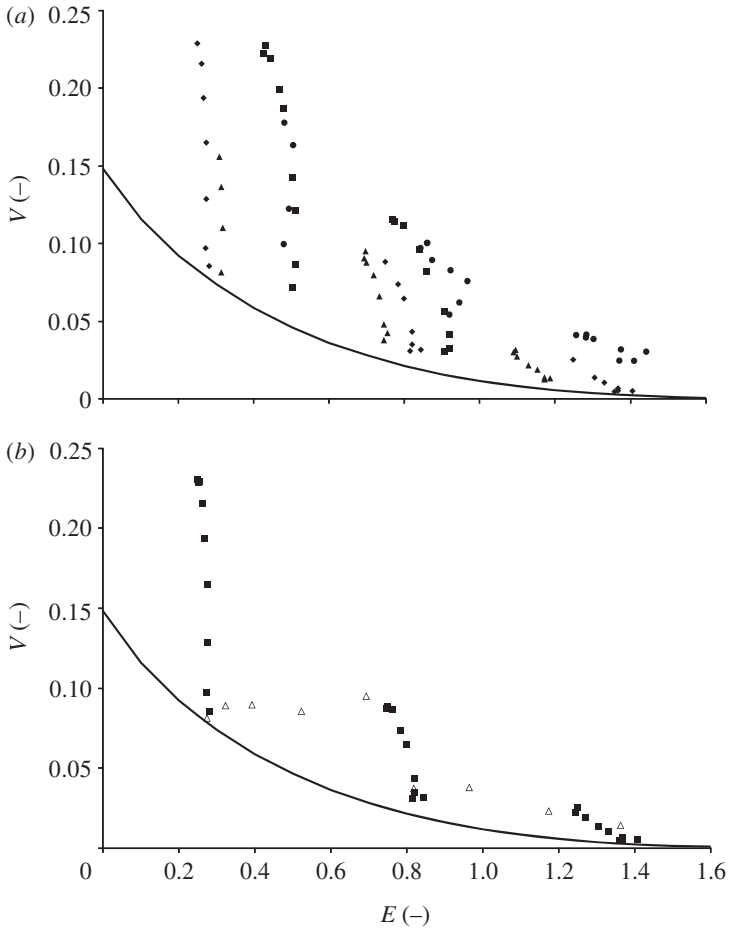

Figure 9. (*a*) Non-dimensional overtopping volume (V) versus non-dimensional truncation elevation (E) for bores. Filled squares, $d = 10.5$ cm; filled diamonds, $d = 15.5$ cm; filled triangles, $d = 21$ cm; filled circles, $d = 26$ cm; solid line, PW01 solution. (*b*) Non-dimensional overtopping volume (V) versus non-dimensional truncation elevation (E) for developed bores and solitary waves for $d = 15.5$ cm. Filled squares, bores; open triangles, solitary waves; solid line, PW01 solution.

behaviour was noted earlier for data from a single water depth in figure 6. In figure 9*a*, clusters also contain data from different water depths. The data show a lower bound consistent with the Peregrine & Williams (2001) solution, but also exceed this solution by up to a factor of four. The contrast between the overtopping data for bores and the non-breaking waves is further illustrated in figure 9*b*, where data from figure 6 are re-plotted using the Peregrine & Williams (2001) scaling. With this scaling, the overtopping rates for the solitary waves and bores again show the opposite behaviour, and are insensitive to E in the former case, and multi-valued for the latter. Again, both wave conditions can result in significantly greater overtopping than that suggested by the Peregrine & Williams (2001) solution.

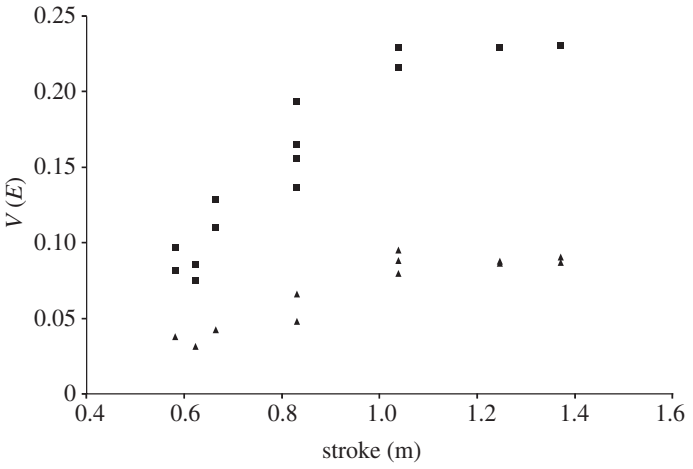

Figure 10. Non-dimensional overtopping volume (V) versus wavemaker stroke length for bores, grouped by relative truncation elevation (E). $d = 0.15$ m and 0.21 m. Filled squares, $E = 0.25$–0.3; filled triangles, $E = 0.7$–0.75.

Figure 10 shows the variation in $V(E)$ with wavemaker stroke length, where the data shown are grouped within two small ranges of E. For $0.25 < E < 0.3$, $V(E)$ is strongly dependent on the stroke length. This is consistent with the data in figures 6 and 9. Hence, the extra mass flux within the bore for different stroke lengths appears as an increase in overtopping volume and not in additional run-up. Thus, while the run-up remains approximately the same for bores of similar height, the flow conditions behind the bore vary significantly with stroke length, leading to different mass and momentum fluxes across the SWL. However, for this wavemaker, increasing the stroke length above a given value ($S \approx 1$ m) does not result in a further increase in the overtopping. This is because the bore propagates away from the wavemaker during the generation process and, for higher bore celerity, the wavemaker ceases to impart further momentum to the fluid behind the bore front. The dependency of V(E) on stroke length reduces for higher truncation positions ($0.7 < E < 0.75$), and is small for $E > 1$. This is because the swash hydrodynamics asymptote to a single solution as the run-up tip is approached, which is discussed shortly.

The multi-valued overtopping rates for a given value of E are entirely consistent with the Guard & Baldock (2007) swash model and the extension of this model to overtopping by Hogg *et al.* (2011). In these solutions, the mass and momentum flux behind the bore are controlled by the free parameter, k; $k = 1$ corresponds to conditions for a uniform incident bore (e.g. Hibberd & Peregrine 1979) and $k = 0$ corresponds to the Shen & Meyer (1963) swash solution. The overtopping rates predicted by the Hogg *et al.* (2011) solution are illustrated for a range of k values in figure 11. V(E) is strongly dependent on k when E is small, with the dependence reducing as E increases, in agreement with the data in figure 11. The dependency on k reduces as $E \to 2$, because the solutions are asymptotic to the Shen & Meyer (1963) and Peregrine & Williams (2001) solutions at the run-up tip. This is because the flow becomes constrained by the shoreline and flow reversal occurs at the same relative time at the run-up tip for all values of k, i.e.

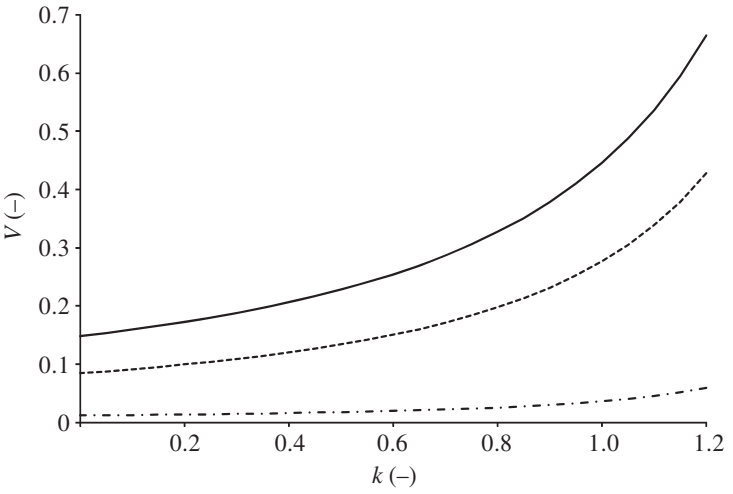

Figure 11. Predicted non-dimensional overtopping volume (V) versus k for varying truncation point, E, for bores (Hogg *et al.* 2011). Solid line, $E=0$, dotted line, $E=0.24$, dashed-dotted line $E=1$.

the shoreline motion always reverses halfway through the swash period and the depth tends to zero at the run-up tip. Guard & Baldock (2007) present contours of flow depth and flow velocity within the swash zone that very clearly illustrate this. It should be noted that the presence of the truncation point increases the shoreward volume flux passing a given elevation on the beach face; i.e. for the same value of k, the Hogg *et al.* (2011) solutions give greater overtopping rates than the integrated shoreward volume flux obtained from the Guard & Baldock (2007) model. This is because the presence of the edge increases the volume flux past a given elevation in comparison with the solution for a non-truncated beach. This might be expected on the basis of a reduction in pressure at the free overfall and hence a reduction in the influence of the adverse pressure gradient that slows the uprush flow.

However, while k describes the asymmetry of the incoming flow to the swash zone, exact values of k have yet to be related to the characteristics of the incident bore. Power *et al.* (2011) showed that natural surf zone bores have flow characteristics that correspond to the range $0<k<1.2$, with a median value of $k\approx 0.8$, and that k was independent of offshore wave height, wave period (or wavelength) and swash period. Further, Power (2011) could not identify a clear correlation between k and inner surf zone wave height, wave period or wave shape. Consequently, k remains as a free parameter in the model. Thus, the model is not yet a fully predictive tool, but we show that the appropriate choice of k provides very good agreement between model and data. Further, we compare the model and data across the full range of truncation locations and for different bores generated with the same stroke length.

Figure 12*a* compares the Hogg *et al.* (2011) model (denoted H11) and data for three bores generated with different (short and long) wavemaker stroke lengths. From fitting to $V(E)$, the respective k values are estimated as $k=0.35$, $k=0.7$ and $k=0.9$, respectively. The solutions (and data) for different k asymptote to the

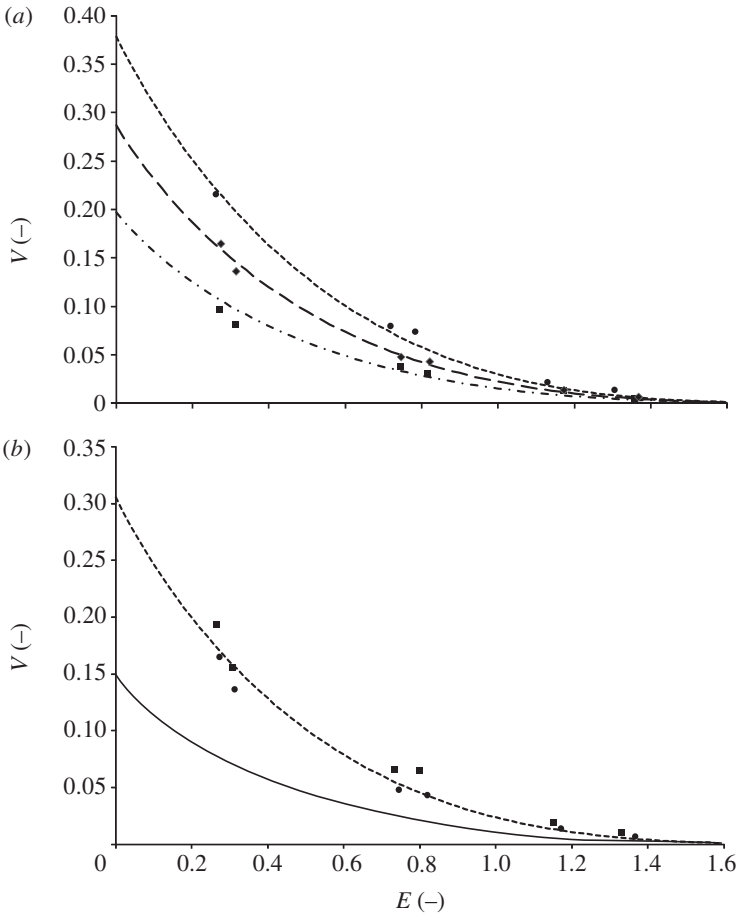

Figure 12. (*a*) Non-dimensional overtopping volume (V) versus E for bores and different wavemaker stroke length, S. Filled squares, $S = 0.58$ m; filled diamonds, $S = 0.84$ m, filled circles, $S = 1.04$ m; solid line, PW01; dashed line, $k = 0.35$; dashed line, $k = 0.7$; dotted line, $k = 0.9$ (H11). (*b*) Non-dimensional overtopping volume (V) versus E for two bores with different wavemaker generation functions and the same stroke length ($S = 0.84$ m). Filled squares, Goring method; filled circles, error function method; dashed line, H11 ($k = 0.75$); solid line, PW01.

Peregrine & Williams (2001) solution as the truncation point approaches the run-up limit ($\mathrm{E} \to 2$), but $V(E)$ is strongly dependent on k closer to the SWL. The solutions accurately describe the variation in overtopping with truncation point that is observed in the data. A similar comparison for two bores with the same stroke but different wavemaker generation functions is illustrated in figure 12*b*, with similar good agreement between model and data. Finally, figure 13 shows the model data comparisons for three bores generated with wavemaker stroke $1.04\,\mathrm{m} < S < 1.38\,\mathrm{m}$, and using both the solitary wave generation method and the error function method. These cases represent conditions where $V(E)$ ceases to increase with stroke length because the wavemaker is no longer capable of imparting further momentum to the flow behind the bore. $V(E)$ is almost identical for each bore, and the variation in $V(E)$ with truncation point is again well described by the model.

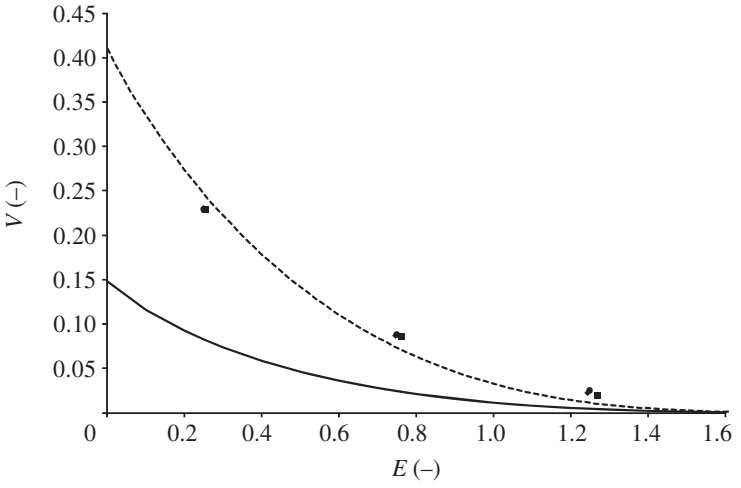

Figure 13. Non-dimensional overtopping volume (V) versus E for three bores at high wavemaker stroke length. Filled circles, $S = 1.04$ m; filled squares, $S = 1.25$ m; filled diamonds, $S = 1.38$ m; dashed line, H11 ($k = 0.95$); solid line, PW01.

5. Conclusions

Experimental data on the overtopping of both solitary waves and solitary bores have been presented. Two different and distinct scaling regimes have been identified for solitary waves and solitary bores. For solitary waves, the dimensional and non-dimensional overtopping volume scales linearly with the deficit in the run-up freeboard and the volume flux in the incident solitary wave. A weak dependence on wave nonlinearity is observed, consistent with the partioning of the volume flux above and below the SWL in the incident wave. For the bores, the overtopping cannot be scaled uniquely because the flow behind the incident bore front is dependent only on the bore height in a special case. However, the data are in very close agreement with recent solutions for the overtopping of long bores derived from the NLSWEs (Hogg *et al.* 2011). For a given run-up deficit, solitary bores transport greater volumes of water across the shoreline than solitary waves. Hence, solitary bores induce greater overtopping than solitary waves when the relative freeboard is small. These results have important implications for tsunami and storm surge hazard management and the design of tsunami evacuation strategies.

D.P. gratefully acknowledges the support of an Australian Postgraduate Award. This work was partially supported by a CSIRO Flagship Cluster Grant under Wealth from Oceans Pipeline Hazards program, the Australian Research Council project LP100100375, which includes support from the Office of Environment and Heritage, NSW and DHI (Australia) and ARC project DP110101176.

References

Antuono, M. & Hogg, A. J. 2009 Run-up and backwash bore formation from dam-break flow on an inclined plane. *J. Fluid Mech.* **640**, 151–164. (doi:10.1017/S0022112009991698)

Baldock, T. E. 2006 Long wave generation by the shoaling and breaking of transient wave groups on a beach. *Proc. R. Soc. A* **462**, 1853–1876. (doi:10.1098/rspa.2005.1642)

Baldock, T. E., Hughes, M. G., Day, K. & Louys, J. 2005 Swash overtopping and sediment overwash on a truncated beach. *Coastal Eng.* **52**, 633–645. (doi:10.1016/j.coastaleng.2005.04.002)

Baldock, T. E., Cox, D., Maddux, T., Killian, J. & Fayler, L. 2009 Kinematics of breaking tsunami wavefronts: A data set from large scale laboratory experiments. *Coastal Eng.* **56**, 506–516. (doi:10.1016/j.coastaleng.2008.10.011)

Barnes, M. P., O'Donoghue, T., Alsina, J. M. & Baldock, T. E. 2009 Direct bed shear stress measurements in bore-driven swash. *Coastal Eng.* **56**, 853–867. (doi:10.1016/j.coastaleng.2009.04.004)

Borrero, J. C. 2005 Field data and satellite imagery of tsunami effects in Banda Aceh. *Science* **308**, 1596. (doi:10.1126/science.1110957)

Borthwick, A. G. L., Ford, M., Weston, B. P., Taylor, P. H. & Stansby, P. K. 2006 Solitary wave transformation, breaking and run-up at a beach. *Proc. Inst. Civil. Eng.-Marit. Eng.* **159**, 97–105. (doi:/10.1680/maen.2006.159.3.97)

Carrier, G. F., Wu, T. T. & Yeh, H. 2003 Tsunami run-up and draw-down on a plane beach. *J. Fluid Mech.* **475**, 79–99.

Chang, Y.-H., Hwang, K.-S. & Hwung, H.-H. 2009 Large-scale laboratory measurements of solitary wave inundation on a 1 : 20 slope. *Coastal Eng.* **56**, 1022–1034. (doi:10.1016/j.coastaleng.2009.06.008)

Dalrymple, R. A. & Rogers, B. D. 2006 Numerical modeling of water waves with the SPH method. *Coastal Eng.* **53**, 141–147. (doi:10.1016/j.coastaleng.2005.10.004)

Dodd, N. 1998 Numerical model of wave run-up, overtopping, and regeneration. *J. Waterway Port Coast. Ocean Eng.* **124**, 73–81. (doi:10.1061/(ASCE)0733-950X(1998)124:2(73))

Donnelly, C., Kraus, N. & Larson, M. 2006 State of knowledge on measurement and modeling of coastal overwash. *J. Coast. Res.* **22**, 965–991. (doi:10.2112/04-0431.1)

Goda, Y. 2009 Derivation of unified wave overtopping formulas for seawalls with smooth, impermeable surfaces based on selected CLASH datasets. *Coastal Eng.* **56**, 385–399. (doi:10.1016/j.coastaleng.2008.09.007)

Goring, D. G. 1979 *Tsunamis: the propagation of long waves on to a shelf*, pp. 337. Pasadena, CA: California Institute of Technology.

Goring, D. & Raichlen, F. 1980 The generation of long waves in the laboratory. In *Proc. 17th Coastal Engineering. Conf., Sydney, Australia, 23–28 March*, pp. 763–784. Reston, VA: ASCE.

Guard, P. A. & Baldock, T. E. 2007 The influence of seaward boundary conditions on swash zone hydrodynamics. *Coastal Eng.* **54**, 321–331. (doi:10.1016/j.coastaleng.2006.10.004)

Hall, J. V. & Watts, J. W. 1953 *Laboratory investigation of the vertical rise of solitary waves on impermeable slopes*. Technical Memorandum 33. Washington, DC: Beach Erosion Board, USACE.

Hedges, T. S. & Reis, M. T. 2004 Accounting for random wave run-up in overtopping predictions. *Proc. Inst. Civil Eng., Maritime Eng.* **157**, 113–122. (doi:10.1680/maen.2004.157.3.113)

Hibberd, S. & Peregrine, D. H. 1979 Surf and run-up on a beach: a uniform bore. *J. Fluid Mech.* **95**, 323–345. (doi:10.1017/S002211207900149X)

Hine, A. C. 1979 Mechanisms of berm development and resulting beach growth along a barier spit complex. *Sedimentology* **26**, 333–351. (doi:10.1111/j.1365-3091.1979.tb00913.x)

Hogg, A. J., Baldock, T. E. & Pritchard, D. 2011 Overtopping a truncated planar beach. *J. Fluid Mech.* **666**, 521–553. (doi:10.1017/S0022112010004325)

Hughes, S. A. & Nadal, N. C. 2009 Laboratory study of combined wave overtopping and storm surge overflow of a levee. *Coastal Eng.* **56**, 244–259. (doi:10.1016/j.coastaleng.2008.09.005)

Hunt-Raby, A. C., Borthwick, A. G. L., Stansby, P. K. & Taylor, P. H. 2011 Experimental measurement of focused wave group and solitary wave overtopping. *J. Hydraul. Res.* **49**, 450–464. (doi:10.1080/00221686.2010.542616)

Ingram, D. M., Gao, F., Causon, D. M., Mingham, C. G. & Troch, P. 2009 Numerical investigations of wave overtopping at coastal structures. *Coastal Eng.* **56**, 190–202. (doi:10.1016/j.coastaleng.2008.03.010)

Kobayashi, N. 1999 Numerical modeling of wave runup on coastal structures and beaches. *Mar. Technol. Soc. J.* **33**, 33–37. (doi:10.4031/MTSJ.33.3.5)

Kobayashi, N. & Wurjanto, A. 1989 Wave overtopping on coastal structures. *J. Waterway Port Coast. Ocean Eng.* **115**, 235–251. (doi:10.1061/(ASCE)0733-950X(1989)115:2(235))

Kobayashi, N., Tega, Y. & Hancock, M. W. 1996 Wave reflection and overwash of dunes. *J. Waterway Port Coast. Ocean Eng.* **122**, 150–153. (doi:10.1061/(ASCE)0733-950X(1996)122:3(150))

Kobayashi, N., Herrman, M. N., Johnson, B. D. & Orzech, M. D. 1998 Probability distribution of surface elevation in surf and swash zones. *J. Waterway Port Coast. Ocean Eng.* **124**, 99–107. (doi:10.1061/(ASCE)0733-950X(1998)124:3(99))

Kraus, N. C., Militello, A. & Todoroff, G. 2002 Barrier breaching processes and barrier spit breach, Stone Lagoon, California. *Shore Beach* **70**, 21–28. (doi:10.2112/SI59-011.1)

Li, Y. & Raichlen, F. 2002 Non-breaking and breaking solitary wave run-up. *J. Fluid Mech.* **456**, 295–318. (doi:10.1017/S0022112001007625)

Madsen, P. A. & Fuhrman, D. R. 2008 Run-up of tsunamis and long waves in terms of surf-similarity. *Coastal Eng.* **55**, 209–223. (doi:10.1016/j.coastaleng.2007.09.007)

Madsen, P. A. & Schaffer, H. A. 2010 Analytical solutions for tsunami runup on a plane beach: single waves, N-waves and transient waves. *J. Fluid Mech.* **645**, 27–57. (doi:10.1017/S0022112009992485)

Madsen, P. A., Fuhrman, D. R. & Schaffer, H. A. 2008 On the solitary wave paradigm for tsunamis. *J. Geophys. Res. Oceans* **113**, C12012. (doi:10.1029/2008JC004932)

Meyer, R. E. & Taylor, A. D. (eds) 1972 *Run-up on beaches. Waves on beaches and resulting sediment transport*, pp. 357–411. London, UK: Academic Press.

Nott, J. F. 2003 The urban geology of Cairns, Queensland, Australia. *Quat. Int.* **103**, 75–82. (doi:10.1016/S1040-6182(02)00142-8)

Orszaghova, J., Borthwick, A. G. L. & Taylor, P. H. 2012 From the paddle to the beach: a Boussinesq shallow water numerical wave tank based on Madsen and Sorensen's equations. *J. Comput. Phys.* **231**, 328–344. (doi:10.1016/j.jcp.2011.08.028)

Parnell, K. E. & Kofoed-Hansen, H. 2001 Wakes from large high-speed ferries in confined coastal waters: management approaches with examples from New Zealand and Denmark. *Coast. Manage.* **29**, 217–237. (doi:10.1080/08920750152102044)

Peregrine, D. H. 1966 Calculations of development of an undular bore. *J. Fluid Mech.* **25**, 321–330. (doi:10.1017/S0022112066001678)

Peregrine, D. H. 1967 Long waves on a beach. *J. Fluid Mech.* **27**, 815–830. (doi:10.1017/S0022112067002605)

Peregrine, D. H. & Williams, S. M. 2001 Swash overtopping a truncated plane beach. *J. Fluid Mech.* **440**, 391–399. (doi:10.1017/S002211200100492X)

Power, H. E. 2011 *Hydrodynamics of surf and swash on natural beaches*, pp. 200. Brisbane, CA: University of Queensland.

Power, H. E., Holman, R. A. & Baldock, T. E. 2011 Swash zone boundary conditions derived from optical remote sensing of swash zone flow patterns. *J. Geophys. Res. Oceans* **116**, C06007. (doi:10.1029/2010JC006724)

Pritchard, D. & Hogg, A. J. 2005 On the transport of suspended sediment by a swash event on a plane beach. *Coastal Eng.* **52**, 1–23. (doi:10.1016/j.coastaleng.2004.08.002)

Pritchard, D., Guard, P. A. & Baldock, T. E. 2008 An analytical model for bore-driven run-up. *J. Fluid Mech.* **610**, 183–193. (doi:10.1017/S0022112008002644)

Ramsbottom, D., Floyd, P. & Penning-Rowsell, E. 2003 Flood risks to people phase 1. R&D Technical Report, FD2317DEFRA DEFRA/Environment Agency. Flood Management Division, London, UK.

Russel, J. S. 1845 Report on waves. In Report of the 14th Meeting of the British Association for the Advancement of Science, pp. 311–390. London, UK: John Murray.

Seelam, J. K., Guard, P. A. & Baldock, T. E. 2011 Measurement and modeling of bed shear stress under solitary waves. *Coastal Eng.* **58**, 937–947. (doi:10.1016/j.coastaleng.2011.05.012)

Shen, M. C. & Meyer, R. E. 1963 Climb of a bore on a beach. III. Runup. *J. Fluid Mech.* **16**, 113–125. (doi:10.1017/S0022112063000628)

Stansby, P. K. 2003 Solitary wave run up and overtopping by a semi-implicit finite-volume shallow-water Boussinesq model. *J. Hydraul. Res.* **41**, 639–647. (doi:10.1080/00221680309506896)

Synolakis, C. E. 1987 The runup of solitary waves. *J. Fluid Mech.* **185**, 523–545. (doi:10.1017/S002211208700329X)

Synolakis, C. E. & Bernard, E. N. 2006 Tsunami science before and beyond Boxing Day 2004. *Phil. Trans. R. Soc. A* **364**, 2231–2265. (doi:10.1098/rsta.2006.1824)

van der Meer, J. W. Verhaeghe, H. & Steendam, G. J. 2009 The new wave overtopping database for coastal structures. *Coastal Eng.* **56**, 108–120. (doi:10.1016/j.coastaleng.2008.03.012)

Weir, F. M., Hughes, M. G. & Baldock, T. E. 2006 Beach face and berm morphodynamics fronting a coastal lagoon. *Geomorphology* **82**, 331–346. (doi:10.1016/j.geomorph.2006.05.015)

Wood, R. M. & Bateman, W. 2005 Uncertainties and constraints on breaching and their implications for flood loss estimation. *Phil. Trans. R. Soc. A* **363**, 1423–1430. (doi:10.1098/rsta.2005.1576)

Yeh, H. 1991 Tsunami bore runup. *Nat. Hazards* **4**, 209–220. (doi:10.1007/BF00162788)

Yeh, H. 2006 Maximum fluid forces in the tsunami runup zone. *J. Waterway Port Coast. Ocean Eng.* **132**, 496–500. (doi:10.1061/(ASCE)0733-950X(2006)132:6(496))

Yeh, H., Liu, P. L.-F. & Synolakis, C. E. (eds) 1996 Long-wave runup models. In *Proc. 2nd International Workshop on Long-wave Runup Models*. Singapore: World Scientific.